Modelling the control of Vestigial and Dll expression by Dpp and Wingless in the Drosophila wing disc

Student: Martin O'Reilly†; Supervisor: Jean-Paul Vincent

This case presentation explores how two key Drosophila morphogens, Decapentaplegic (Dpp) and Wingless (Wg), control the expression of two wing disc transcription factors, Vestigial (Vg) and Distalless (Dll). Two simple models for the potential control of Vg and Dll expression by Dpp and Wg in the mature steady state Drosophila wing pouch are explored. Firstly, a model based on the activation mechanism for Dll in the leg disc was evaluated and dismissed. Secondly, a simple caricature model of Vg activation, based on different thresholds for the contribution of Dpp and Wg to Vg activation, is explored. Although it is limited to modelling the effects of Dpp and Wg, and ignores many other elements later identified as critical to the Vg regulatory pathway, initial analysis suggests that it may be possible to model Vg distribution in the mature wing pouch relatively well using such a simplified steady state model. Further analysis is required to validate the model as it has so far only been assessed against the data used to fit the model parameters. A fuller system of Vg development is then described and the implications for modelling this more complex system discussed.

Introduction

Decapentaplegic (Dpp) and Wingless (Wg) are two key morphogens controlling the development of leg and wing appendages in Drosophila. This case essay explores how the distribution of these morphogens in the Drosophila wing pouch controls the expression of two downstream transcription factors Vestigial (Vg) and Distalless (Dll).

Two simple mechanisms for the potential control of Vg and Dll expression by Dpp and Wg in the mature steady state Drosophila wing pouch are explored. Firstly, a model based on the activation mechanism for Dll in the leg disc is evaluated. Secondly, a simple caricature model of Vg activation, based on different thresholds for the contribution of Dpp and Wg to Vg activation, is explored. Although it is limited to modelling the effects of Dpp and Wg, and ignored many other elements identified as critical to the Vg regulatory pathway, initial analysis suggests that it may be possible to model Vg distribution in the mature wing pouch relatively well using such a simplified steady state model.

The full complexity of the Vg regulatory pathway in wing development is then discussed, as well as the impact of complex morphogen transport on modelling. Potential difficulties in determining morphogen signalling levels from measured morphogen levels are also examined. Finally, the issues of modelling such a complex time-varying system for Vg activation are addressed, especially the requirement for substantial qualitative data to constrain the model parameters.

Background

All adult tissue in Drosophila develops from groups of epithelial cells called imaginal discs. These discs form in the embryo and develop extensively during the larval stage. In each of the three thoracic segments of the embryo and larva there is a pair of ventral imaginal discs which form each of the three pairs of legs in the adult fly. In the central and posterior thoracic segments, there are also pairs of dorsal discs which respectively form the wings and halteres[1] in the adult fly (see figure 1). Successful development of both leg and wing imaginal discs into their respective adult organs is critically dependent on the expression of Dpp and Wg within the discs.

Vg is crucial for the proper development of the wing disc and is widely considered to be the primary marker of wing fate. Wing discs in which Vg expression is repressed fail to develop at all and the ectopic expression of Vg in leg imaginal discs results in ectopic production of wing tissue (Kim et al 1996).

Dll is crucial to the proper development of the leg disc but appears much less important for wing disc development. However, expression of Dll in both leg and wing discs is centred on an area of overlapping high levels of Dpp and Wg expression, and Dll expression in the wing is almost concentric with the expression of Vg. Therefore the regulation of Dll by Dpp and Wg in the wing is considered here for comparison with its regulation in the leg and its relation to regulation of Vg in the wing.

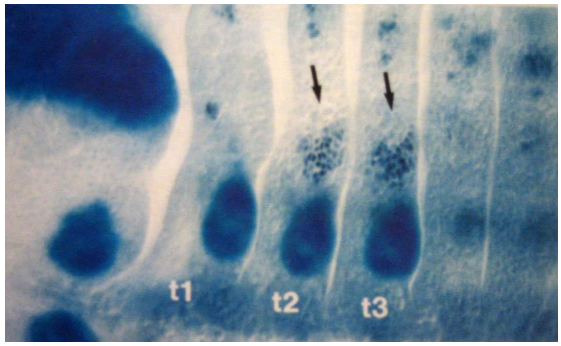

Figure 1: Wing and leg imaginal discs in a late stage 12 Drosophila embryo. The thoracic segments are marked t1-t3 and the leg imaginal discs are the large, dark stains directly above these markers. The wing imaginal discs are the smaller, more patchy stains indicated by the arrows. *[Source: Bate and Martinez-Arias, 1993]*

The question

The problem this case essay will explore is how the observed distributions of Vg and Dll in the wing pouch of the wing imaginal disc might be explained by the observed distributions of Dpp and Wg. The wing pouch is a ventrally located, approximately oval

[1] Halteres are small wing-like structures. They can be made to develop into full-blown wings by the suppression of Ultraborax (Ubx) expression in the haltere disc during development.

† MRes student at UCL CoMPLEX (Centre for Mathematics and Physics in the Life Sciences and Experimental Biology).
Email: martin.o'reilly@ucl.ac.uk

sub-section of the imaginal disc which develops into the wing proper. The remainder of the disc develops into the wing hinge and the notum (part of the fly body). Dpp and Wg are both required for the expression of Dll and Vg and over-expression of either Dpp or Wg will result in increased Vg and Dll expression.

Dpp is expressed in a stripe of cells along the anterior-posterior (A-P) compartment boundary within the wing imaginal disc and Wg is expressed in a narrower, orthogonal stripe of cells along the dorsal-ventral (D-V) compartment boundary. While production of each morphogen is restricted to its respective stripe of source cells, Dpp and Wg spread outwards from these source stripes, forming decaying gradients of morphogen. Typical Dpp and Wg distributions are shown in figure 2. The two discs images are not to the same scale, and the wing pouch in each disc is outlined for reference.

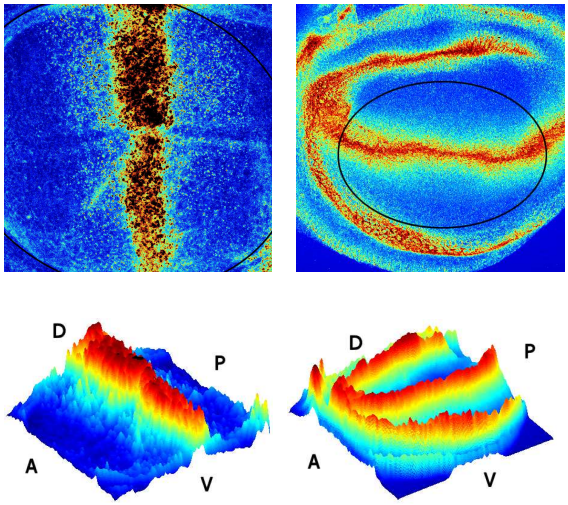

Figure 2: Distributions of Dll (left column) and Wg (right column) in 2 different wing discs. Top plots are 2D "heat maps" depicting morphogen levels as colour changes from blue (zero) to red (maximum level recorded for disc). Black pixels indicate where the original image data was saturated and therefore there is uncertainty regarding the true morphogen level at that point. Only the Dpp stains suffered from significant saturation. Extent of wing pouch is indicated with black oval to provide a common scale and reference across plots. Bottom plots show the same data in 3d after Gaussian smoothing. See methods section for more detail on disc image data processing. See appendix for more detail on image processing and visualisation.

Vg and Dll are both expressed in approximately horizontal bands centred on the Wg source stripe at the D-V boundary. Vg is expressed in cells across the entire wing pouch, while Dll expression is restricted to a subset of wing pouch cells closer to the D-V boundary (see figure 3). The key question explored by this case essay is how the cross-like pattern of combined Dpp and Wg expression can give rise to the horizontally elongated but much more symmetric distributions of Vg and Dll.

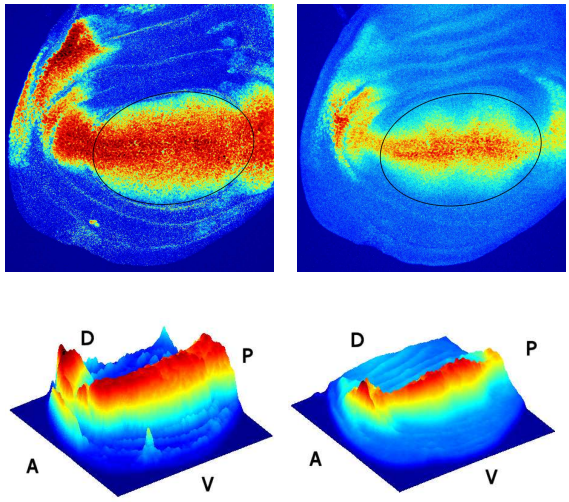

Figure 3: Distributions of Vg (left column) and Dll (right column) in the same wing disc. Top plots are 2D "heat maps" and bottom plots show smoothed 3D plots of the same data. Extent of wing pouch is indicated with black oval in 2D plots. Image data processed as for plots in fig 2.

Potential simple answers

A separate regulator driven by Dpp and Wg

It is possible that the observed pattern of Vg and Dll expression might arise if both were driven by a separate regulator for which activation was initially triggered by high levels of both Dpp and Wg but then spread outwards from its initial source.

Vg is not expressed in the leg. However Dll is and its expression profile there is, as in the wing, centred on an area of overlapping high levels of Dpp and Wg (see figure 4). Recently just such a regulator proposed above may have been uncovered for Dll expression in the leg. The leg trigger (LT) element, located close to the site of Dll transcription initiation, shows high levels of expression in the area of Dpp/Wg overlap and has binding sites for both Dpp and Wg downstream targets. A separate maintenance element (M) was found to be able to maintain Dll expression in the absence of Dpp and Wg, but only when in cis to the LT element (Estella and Mann, 2008).

It is tempting to imagine that the same mechanism might be at work in the wing disc, causing the observed centring the of the Dll expression profile on the intersection of Dpp and Wg expression. However, there are a few problems with this model. Firstly, the expression of Dll driven by this mechanism in the leg disc results in a spherically symmetric distribution of Dll, yet the observed distribution in the wing is extended along the D-V boundary. While a preferential expansion of the growing disc along the D-V boundary could explain the stretching of an initially symmetric Dll distribution, the opposite is in fact observed and clones induced in the wing disc are stretched *perpendicular* to the D-V boundary (Desplan and Lecuit, 2003). Secondly, there is no evidence that either Dll or the LT/M pathway regulates Vg expression. In fact, the available evidence suggests that the opposite is true and that expression of Dll in the wing is triggered by Vg (Klein and Martinez-Arias,

1999). Finally, LT expression was tested for in wing discs by Estella and Mann (2008) and was not found to be present. It is therefore extremely unlikely that either Vg or Dll expression in the wing disc is driven by the same mechanisms as Dll expression in the leg disc.

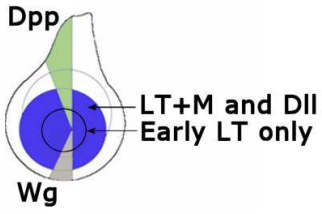

Figure 4: Expression of Dpp, Wg and Dll in the leg imaginal disc. LT is initially expressed in the central region of the disc, where Dpp and Wg levels are both high, and drives initial high levels of Dll expression in this area. Dll expression then expands to cover the entire blue zone, overlapping expression domain of the cis-regulatory composite element LT+M.

Unequal dependence on Dpp and Wg

Another possibility is that the observed distribution of Vg and Dll might arise if expression was primarily determined by the level of Wg, with Dpp expression required at a much lower "permissive" level. This was explored using a caricature model of Vg activation. In this model Vg expression was calculated by specifying a separate sigmoidal threshold function for each morphogen using a suitable Naka-Rushton equation (see equation 1 and figure 5). The parameter n controls the steepness of the function and the parameter c_{50} sets the point at which the output of the function is 0.5. In the model a partial contribution to Vg activity for each morphogen was calculated by passing the morphogen level at each point through its individual threshold function. The level of Vg activity in the model was then determined by multiplying together the partial contributions for the two morphogens, representing a synergistic interaction of Dpp and Wg.

$$R = R_{\max}\frac{c^n}{c^n + c_{50}^n} \quad \text{(Equation 1)}$$

In the initial proof of concept model Dpp and Wg producing cells were modelled as perpendicular stripes of 2 and 12 cells respectively (based on the relative sizes of the stripes in the disc image data). Dpp and Wg levels away from the source were modelled as exponential decays with length constants of 5.5[2] and 7.7 cells respectively (from Kicheva et al, 2007) and minimum morphogen levels were set from the disc image data provided for this case essay. The choice of exponential decay to model steady state morphogen distributions was based on the assumption that transport of Dpp and Wg can be modelled using a diffusion equation where neither the diffusivity nor the degradation rate varies with position or morphogen level. It should be noted that neither Dpp nor Wg transport actually appear to be via passive diffusion but it seems that, at least to a first approximation, both morphogen gradients can be represented by exponential decays.

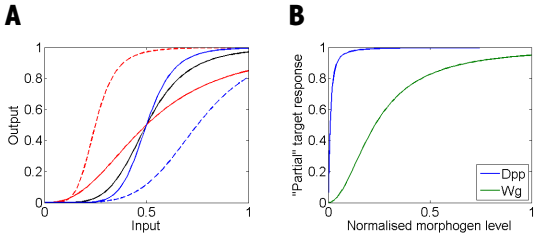

Figure 5: **A:** Representative Naka-Rushton response functions illustrating the effect of varying values of parameters n (solid lines) and c_{50} (dashed lines). Black curve represents a reference parameter set and red and blue curves represent a decrease or increase in the parameter respectively. **B:** Sigmoidal "partial" response functions used in the caricature "permissive Dpp" model.

In order to produce a Vg distribution that was qualitatively similar to that observed in the wing pouch, the c_{50} parameter for Dpp had to be set near or below the minimum level of Dpp observed in the wing disc. This was effectively equivalent to turning the Dpp element of the Vg activation mechanism on throughout the wing pouch and produced an elongated "ridge" of Vg activity oriented along the D-V boundary (see figure 6A). The width of the ridge and its gradient along the A-P boundary could be adjusted by varying the c_{50} and n parameters for the Wg threshold function respectively.

The model was then adjusted to use real Dpp and Wg distributions taken from the disc images provided for this case essay. As there was no triple Dpp/Wg/Vg stain, it was necessary to combine a dual Wg/Vg stain with a separate Dpp stain from another disc. The Dpp image data was rescaled and realigned so that its wing pouch overlapped the wing pouch in the Wg/Vg disc. The Wg threshold parameters in the model were then adjusted by eye to fit the observed Vg distribution, and the result can be seen in figure 6B. The model prediction is a reasonable fit to the observed data, although the Vg ridge is somewhat broader in the real data than in the model.

As the observed Vg distribution was used to fit the model parameters, this result can only be taken as an indication that it is possible to relate observed Dpp and Wg distributions reasonably well to observed Vg distribution using a model of this form. In order to determine if this model has predictive power it will be necessary to evaluate how well it predicts the observed Vg distribution from Dpp and Vg levels in other discs using the same parameter values. For this evaluation the validation discs should be triple stained for Dpp/Wg/Vg to minimise any error or artefacts introduced by the scaling and alignment process required to merge data from two different discs. The error between the predicted and observed Vg expressions should also be quantified using an appropriate metric, rather than qualitatively evaluated by eye as it was for this initial model exploration. Prior to validation, the model parameters should also be more robustly determined by performing an automated fit across several triple

[2] The Wg length constant in the Kicheva experiments was measured by expressing Wg in the wing Dpp domain. This would give it a wider source stripe than normal. However, provided Wg transport can be effectively modelled by a diffusion equation where neither the diffusivity (D) nor the degradation rate (k) varies with position or Wg level, this would not affect the measured length constant (determined by the square root of D/k).

stained discs which are distinct from the set to be used for model validation.

It is not clear whether the low threshold for the Dpp element of Vg activation required in the model is biologically plausible. The evidence presented in Kim et al (1997) for the role of Dpp (via Mad) in the activation of Vg is not quantitative and cannot provide any real indication of the level of Mad required for this element of Vg activation. However, given that the region of Vg expression extends right up to the edges of the wing pouch, it is not unreasonable to suppose that the level of Mad (and hence Dpp) required for Vg activation is close to or below the minimum observed within the wing pouch.

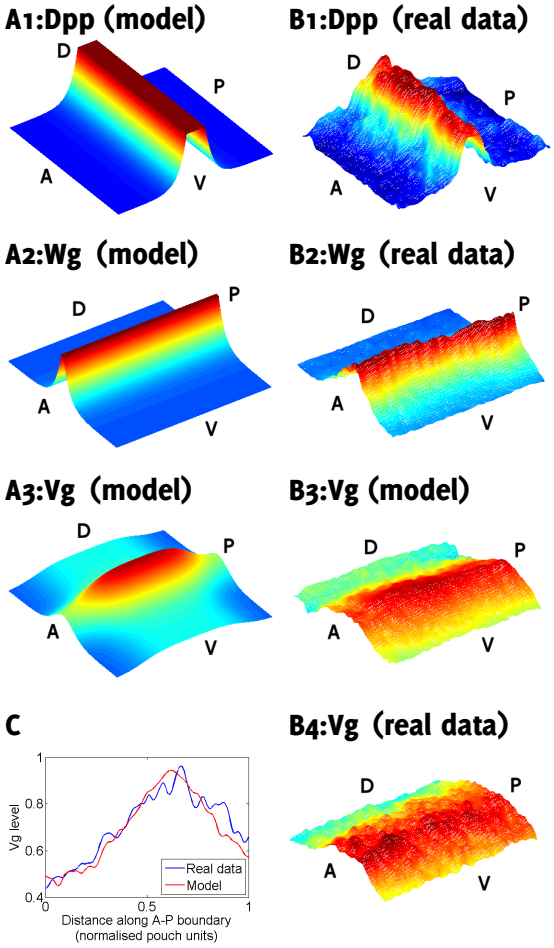

Figure 6:.Output of caricature "permissive Dpp" model. **Plots A1-3:** Caricature distributions of Dpp and Wg (modelled by perpendicular uniform width source stripes with exponential decay). **Plots B1-4:** Real distributions of Dpp and Vg used as inputs to the model with the same parameters as plots. B3 shows the Vg distribution predicted by the model and B4 shows the actual Vg distribution observed in the disc. **Plot C:** Cross-sections of Vg model and real distributions taken along the A-P boundary.

The complex answer

The model discussed above may or may not be able to usefully predict the expression of Vg in the wing pouch from observed distributions of Dpp and Wg. However, its explanatory power is likely to be limited beyond suggesting that the role of Dpp in Vg activation is probably permissive in nature. In the best case, the model would provide an excellent fit to the observed data. Even then it would say nothing about the mechanism of Vg activation other than it is strongly modulated by Wg levels. In fact, much is known about the activation of Vg in the wing pouch and it is known to depend on the interaction of several elements including, but not limited to, Wg and Dpp.

Vg activation is driven by many complex interactions

The activation of Vg is a complicated process, involving a range of different signals at different points in wing disc development.

1. In early wing disc development (prior to the formation of the D-V boundary). Wg is expressed in the ventral part of the wing disc. This heritably represses the expression of Teashirt (Tsh) in this region and this area defines the future wing pouch. Vg is also expressed in the anterior ventral region of the disc at this early stage, overlapping considerably with the region of Wg expression (Wu and Cohen, 2002).

2. At about the same time, the expression of Apterous (Ap) is heritably activated in the dorsal part of the wing disc, defining the dorsal compartment (Klein, 2001). Wg and Ap expression overlap at the D-V boundary and trigger the initiation of Delta/Serrate/LAG-2 (DSL-Notch) signalling between cells either side of this boundary (Zecca and Struhl, 2007).

3. DSL-Notch signalling at the D-V boundary induces the expression of Wg and Vg. The expression of Vg is driven by the combined effect of Wg and DSL-Notch signalling on the vestigial boundary enhancer (vgBE), which then promotes Vg expression (Kim et al, 1995; Klein and Martinez-Arias, 1999).

4. The expression of Vg at the DV boundary then drives the expression of Vg in neighbouring cells, via the vestigial quadrant enhance (vgQE). The vgQE is activated by a combination of Wg, Vg and Mad (itself activated by Dpp). The vgQE is repressed by DSL-Notch signalling and hence is only active away from the D-V boundary. The expression of Vg is then triggered in a cell to cell cascade via the vgQE, with Vg activation levels modulated by the levels of Wg and Vg experienced by each cell, resulting in decreasing expression with increasing distance from the D-V border. Intriguingly, this feedforward pathway also relies on pre-existing low levels of Vg expression in the cells to be recruited to the Vg expression domain, under the control of a separate "priming" enhancer. Vg is additionally constrained to the presumptive wing pouch as identified by the earlier repression of Tsh (Kim et al, 1997; Zecca and Struhl, 2007 and 2007a). Furthermore, the contribution of Dpp to Vg activation via Mad may itself require the co-operative action of yet another transcription factor, Drifter (Certel et al 2000).

Dpp and Wg transport are not via passive diffusion

Neither Dpp nor Wg transport appears to be via passive diffusion. Due to a dependence of Dpp transport on dynamin, it has been suggested that Dpp may be transported via a transcytosis mechanism. In

transcytosis, morphogen is absorbed into and recycled out of cells via endocytosis, resulting in a trafficking of Dpp *through* cell bodies (Vincent and Dubois, 2002; Kicheva et al 2007). However, assuming transcytosis activity is independent of position and Dpp level, it could still be modelled using a diffusion equation with fixed diffusivity and degradation terms and could therefore be modelled as an exponential decay in the steady state. Indeed Kicheva et al (2007) found that the Dpp gradient was fitted well by an exponential distribution.

Wg transport is dynamin independent (Strigini and Cohen 2000; Kicheva et al 2007), although it has been proposed that Wg diffusion is mediated by glypicans on the cell surface, due to the fact that over-expression of the glypican Dally-like (Dlp) results in increased levels of Wg. There is some evidence that the steady state Wg gradient is not well modelled by an exponential and is better fitted by a diffusion model in which the degradation rate of a morphogen-glypican complex depends on the morphogen level (Hufnagel et al, 2006). However, Kicheva et al (2007) claim that the Wg gradient is well fitted by an exponential decay, and initial analysis of data from the wing disc images supplied for this case essay also show that the Wg gradient is at least fairly well approximated by an exponential decay. The Hufnagel and Kicheva plots of the Wg gradient are shown in figure 7, alongside a representative fit from a Wg stain provided for this case essay.

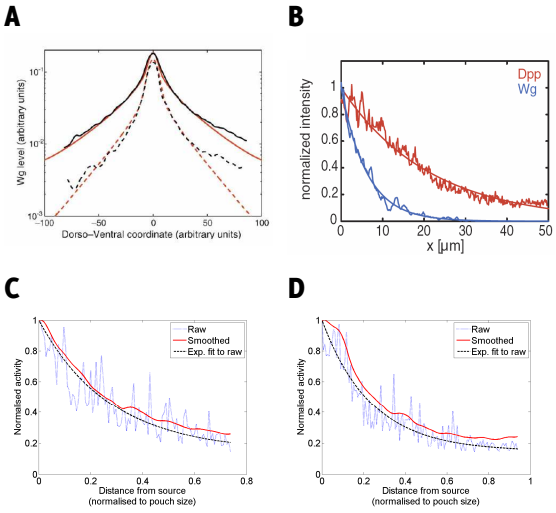

Figure 7: Comparison of various fits to the Wg gradient. **Plot A:** Wingless gradients from 2 wing discs (black solid and dashed lines) plotted on a semi-log axis alongside model the predictions of the Hufnagel model (red solid and dashed lines). It can be seen that in these experiments the Wg gradient is not exponential and the model provides a better fit to the data *[Source: Hufnagel et al, 2006)]* **Plot B:** Exponential fits to Dpp (blue) and Wg (red) gradients in another experiment, where it can be seen that the Wg gradient appears to be fitted well by an exponential *[Source: Kicheva et al, 2007)]* **Plots C-D:** Representative exponential fits (black) to raw Wg gradients (blue) from two nearby cross-sections of the same disc. Red lines show the Wg gradient for each cross-section following Gaussian smoothing of the disc image data. It can be seen that there is significant variation in the raw data and that the exponential fit is a reasonable fit to the raw data and tracks the smoothed data quite closely *[Source: disc data provide for this case essay]*

The precise mechanisms of morphogen transport are not important for models that use real steady state morphogen level data as inputs, such as the simple model explored above. However, they may be important for models incorporating the temporal development of morphogen activity. If any downstream targets of a morphogen change their expression levels faster than it takes the morphogen gradient to reach a steady state, any interpolation of morphogen levels between time points will require an appropriate transport model.

Dpp and Wg levels may not reflect morphogen activity

While increased Dlp expression results in increased levels of Wg across the disc, its effect on Wg activity as measured by Dll expression is more complicated. Away from the D-V boundary increased levels of Dlp result in increased levels of Dll, as would be expected from a general increase in Wg levels. However, despite an increase in Wg activity, Dll levels near the D-V boundary are reduced (Baeg et al, 2004; Hufnagel et al, 2006). This effect is illustrated in figure 8 and, in the Hufnagel model, is attributed to the degradation of a Dlp-Wg complex being dependent on the level of Wg signalling. Additionally, increased expression of DFrizzled2 (DFz2), a Wg receptor, is associated with increased levels of extracellular Wg but decreased levels of intracellular Wg, implying a reduction in Wg uptake (and therefore signalling) in the presence of increased Wg levels (Baeg et al, 2004). With such interactions possible between a morphogen and its receptors and mediators, it is not at all clear that measured morphogen levels accurately reflect underlying morphogen signalling activity.

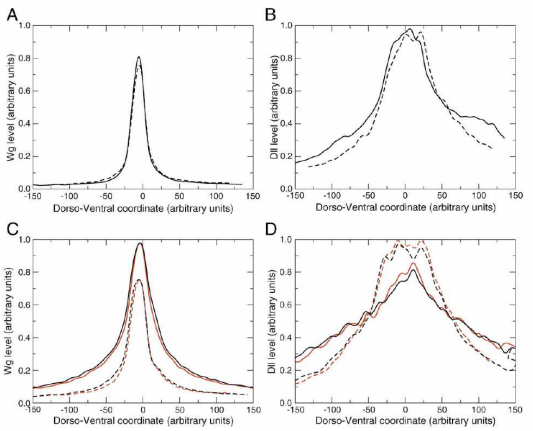

Figure 8: The effect of raised Dlp levels on Wg and Dll expression. Red and black lines represent two different discs. Solid lines are cross-sections from the posterior compartment and dashed lines from the anterior compartment. Plots A-B: Expression in wild-type, Plots C-D: Expression in a mutant where Dlp is over-expressed in the posterior compartment (solid lines). It can be seen that increased Dlp expression results in an approximately uniform increase in Wg expression. However, Dll the effect on Dll is more complex, being repressed near to the D-V boundary and enhanced far away from it *[Source: Hufnagel et al, 2006)]*

Further work

Improved modelling

It is clear that Vestigial expression is governed by a far more complex system of interactions than the simple Dpp/Wg interaction modelled for this case essay. This system will require a correspondingly more detailed and complex model. It may be possible to develop a relatively simple steady state model of Vg expression in the mature wing disc, based on the steady state distributions of the various elements involved in the Vg regulatory pathway at this late stage. However, it seems clear that the development of Vg expression is an inherently dynamic process and would be more suitably described by a model in which the expression of each element evolves over time under the influence of the elements it interacts with. A system of differential equations may be one suitable model to encompass the time dependent interactions of the various elements comprising the Vg regulatory pathway.

More complex models will have more parameters and thus require more detailed and quantitative data to constrain them sufficiently. Even a useful steady state model will require that the relative activation levels of each element are known. This will require calibration of scans to map specific levels of target activation to specific levels of intensity for each target. A useful model encompassing the time dependent nature of the interactions between Vg regulatory elements will require even more parameters and correspondingly greater data. Specifically it will require accurate measures of the activity of each element at various stages of development. Given the above discussion regarding the potential mismatch between morphogen levels and signalling activity, correct parameter estimation in either model may also require a better indicator of morphogen signalling activity.

Manipulation of 3D volume data

It is possible that intracellular morphogen levels might be a more accurate indicator of morphogen activity than total or extracellular levels. It would therefore be useful to separately analyse the distributions of intra and extracellular morphogen. This may be possible via specific staining techniques (e.g. staining for extracellular Wg) or via staining of cell membranes and/or nuclei. It is not clear if a staining technique such as that used to mark extracellular Wg can separately mark intra and extra cellular target in the same stain. However, a cell membrane stain might potentially permit the automatic segmentation of cell interiors from the 3D image data, which could then allow the separate measurement of intra and extra-cellular morphogen levels. Although such automated segmentation will not be straightforward, algorithms exist that can perform the analogous 2D task with suitable quality images. Identification of cell boundaries might also permit more intelligent smoothing techniques which average activity on an individual cell level.

Better time course data

In order to understand and model the complex development of Vg expression in the wing pouch it would be useful to have good data on the time-course of the development of each species implicated in the activation of Vg. Some data already exists on the general distribution of various combinations of species at key stages of development (see Wu and Cohen, 2002 for example). However, to accurately model the temporal development of the Vg regulatory system, the relative activation of each of its elements must be quantitatively known at key time points in development. The spacing of time points required to accurately model the time course of development must be sufficiently close that it is possible to reliably interpolate any changes in the activity of regulatory elements occurring between them.

While a reasonably full picture of the relative distribution of all species at each time point might be constructed from a suitable mix of stains and time points from different discs, a much fuller picture could be painted if the full development of single discs could be tracked. This would involve monitoring several target species in-vivo through the entire development of the larval wing disc as the wing pouch grows from 40 cells to 50,000 cells. If snapshots could be taken at least once per cell division (approximately 10 in total) it may be possible to piece together the full history of each cell in terms of its expression of target species.

However, even taking 10 snapshots during disc development is no small task. Firstly the requirement for in-vivo monitoring would require all target species to be tagged with separable fluorescent markers so that the activity of each species can be independently measured. With available markers and florescence microscope systems it should be theoretically possible to monitor around 4 species simultaneously. This compares favourably to the number of stains observed in single fixed discs in the literature but will rely on the availability of a suitable range of florescent markers. It is not clear if the current range of markers will permit arbitrary combinations of species to be monitored together.

Secondly, and more crucially, live larvae move. Paralysing the larva for imaging is an extremely stressful event and it is unlikely that a larva would survive this 10 times and develop normally. Recently a researcher has used real-time target tracking to centre a continuous microscopy scan on a small volume around a motile bacterium. It may be possible to use a similar technique to track the wing disc within the larva and scan it without paralysing it. However, this depends on being able to scan the disc sufficiently quickly to avoid motion blur. It seems likely that, as the disc grows, some kind of trade off between scan speed and spatial resolution would need to be made to ensure the disc images do not suffer motion blur. It is therefore not clear whether cell-level resolution could be maintained throughout disc development.

Exploration of cell mechanics

In an ideal scenario, snapshots could be taken frequently enough that the movement of individual cells in the disc could be tracked throughout development. Comparatively little is known about the role of cell mechanics in the development of the wing, yet it is clear that it plays an important role. For example, the cells comprising the anterior compartment of the wing disc are physically kept from mixing with those comprising the posterior compartment by changes to cell-cell adhesion properties triggered by the action of engrailed (Bate and Martinez-Arias, 1993). Dorsal and ventral compartment cells are prevented from intermingling by a similar mechanism. Additionally, it is known that clones induced in wing discs expand preferentially in the proximal-distal direction, and it is thought that

the cells divide along random axes and then preferentially rearrange themselves along this axis (Desplan and Lecuit, 2003). Finally, it has been shown that Wg regulates a cell-cell adhesion protein called DE-Cadherin, establishing a proximal-distal gradient of cell-cell adhesion, which plays a role in patterning along this axis (Jaiswal et al, 2005). It is quite possible that this adhesion gradient makes the most proximal portion of the wing disc most likely to "pop out" of the disc plane under the compressive forces generated by cell proliferation, driving the formation of an appropriately shaped wing. However, given the difficulty inherent in even taking even a modest number of in-vivo snapshots during larval development, it is unlikely that snapshots could be taken sufficiently frequently to permit unambiguous tracking of cell movement.

Conclusion

Two simple mechanisms for the potential control of Vg and Dll expression by Dpp and Wg in the mature steady state Drosophila wing pouch were explored. Firstly, a model based on the activation mechanism for Dll in the leg disc was evaluated. It was dismissed primarily due to the fact that a key element of this activation pathway is not expressed in the wing disc. Additionally, the leg disc activation model fails to explain the observed difference in the horizontal and vertical extent of the Dll distribution observed in the wing disc. Secondly, a simple caricature model of Vg activation, based on different thresholds for the contribution of Dpp and Wg to Vg activation, was explored. Although it was limited to modelling the effects of Dpp and Wg, and ignored many other elements identified as critical to the Vg regulatory pathway, initial analysis suggests that it may be possible to model Vg distribution in the mature wing pouch relatively well using such a simplified steady state model. Further analysis is required to validate the model as it has so far only been assessed against the data used to fit the model parameters.

It is clear that the simplified model explored in this case essay is not especially informative, given what is known about the complex range of interactions contributing to Vg activation in the wing pouch. The development of Vg expression during development is clearly a dynamic process, and it is suggested that a more refined model is produced that can capture the time-varying interactions of the various elements comprising the Vg regulatory pathway. Such a complex model will require substantially more quantitative data in order to constrain their parameters. Obtaining this data will require calibrated imaging throughout wing pouch development in order to determine how the relative levels of the each of the Vg regulatory elements varies over this time. Ideally these will be monitored in-vivo over the development of single discs. However, this will be technically challenging and it may only be possible to obtain data for different time points from different discs. In this case, suitable calibration of activity level reporters should permit the amalgamation of data from different discs.

Finally, if the substantial technical hurdles of in-vivo imaging at a large number of time points can be overcome, high temporal resolution data tracking disc development may provide some insight into the role of cell mechanics in this process.

Acknowledgements

Thanks to Jean-Paul Vincent for proposing the topic for this case essay and his advice and guidance during his supervision of it. Thanks also to Eugenia Piddini, Alberto Baena-Lopez and Anna Kicheva for providing disc image data and guidance on disc development and image interpretation. Thanks finally to Xavi Franch Marro for providing disc image data.

UCL CoMPLEX is an EPSRC-funded Life Sciences Interface Doctoral Training Centre.

References

Baeg, G.H.; Selva, E. M.; Goodman, R. M.; Dasgupta, R. & Perrimon, N. (2004). The Wingless morphogen gradient is established by the cooperative action of Frizzled and Heparan Sulfate Proteoglycan receptors. Developmental Biology *276*, 89 - 100.

Bate, M. & Arias, A. M. (1993). The Development of Drosophila melanogaster (vol II). Cold Spring Harbour Laboratory Press.

Certel, K.; Hudson, A.; Carroll, S. & Johnson, W. (2000). Restricted patterning of vestigial expression in Drosophila wing imaginal discs requires synergistic activation by both Mad and the drifter POU domain transcription factor. Development *127*, 3173-3183.

Desplan, C. & Lecuit, T. (2003). Developmental biology: Flowers' wings, fruitflies' petals. Nature *422*, 123-124.

Estella, C.; McKay, D. J. & Mann, R. S. (2008). Molecular Integration of Wingless, Decapentaplegic, and Autoregulatory Inputs into Distalless during Drosophila Leg Development. Developmental Cell *14*, 86 - 96.

Hufnagel, L.; Kreuger, J.; Cohen, S. M. & Shraiman, B. I. (2006). On the role of glypicans in the process of morphogen gradient formation. Developmental Biology *300*, 512 - 522.

Jaiswal, M.; Agrawal, N. & Sinha, P. (2006). Fat and Wingless signaling oppositely regulate epithelial cell-cell adhesion and distal wing development in Drosophila. Development *133*, 925-935.

Kicheva, A.; Pantazis, P.; Bollenbach, T.; Kalaidzidis, Y.; Bittig, T.; Julicher, F. & Gonzalez-Gaitan, M. (2007). Kinetics of Morphogen Gradient Formation. Science *315*, 521-525.

Kim, J.; Irvine, K. D. & Carroll, S. B. (1995). Cell recognition, signal induction, and symmetrical gene activation at the dorsal-ventral boundary of the developing drosophila wing. Cell *82*, 795 - 802.

Kim, J.; Johnson, K.; Chen, H. J.; Carroll, S. & Laughon, A. (1997). Drosophila Mad binds to DNA and directly mediates activation of vestigial by Decapentaplegic. Nature *388*, 304-308

Klein, T. (2001). Wing disc development in the fly: the early stages. Current Opinion in Genetics & Development *11*, 470 - 475.

Klein, T. & Martinez-Arias, A. (1999). The vestigial gene product provides a molecular context for the interpretation of signals during the development of the wing in Drosophila. Development *126*, 913-925.

Ng, M.; Diaz-Benjumea, F. & Cohen, S. (1995). Nubbin encodes a POU-domain protein required for proximal-distal patterning in the Drosophila wing. Development *121*, 589-599.

Strigini, M. & Cohen, S. M. (2000). Wingless gradient formation in the Drosophila wing. Current Biology *10*, 293 - 300.

Vincent, J.P. & Dubois, L. (2002). Morphogen Transport along Epithelia, an Integrated Trafficking Problem. Developmental Cell *3*, 615-623.

Wu, J. & Cohen, S. M. (2002). Repression of Teashirt marks the initiation of wing development. Development *129*, 2411-2418.

Zecca, M. & Struhl, G. (2007). Recruitment of cells into the Drosophila wing primordium by a feed-forward circuit of vestigial autoregulation. Development *134*, 3001-3010.

Zecca, M. & Struhl, G. (2007b). Control of Drosophila wing growth by the vestigial quadrant enhancer. Development *134*, 3011-3020.

Appendix

Methods

Data processing

Raw data from 3D confocal microscopy scans of stained wing discs from late 3rd instar larvae were provided by Eugenia Piddini (2 dual Vg and Dll stains plus one separate stain for each); Alberto Baena-Lopez (15 dual Wg and Vg stains); Anna Kicheva (3 Dpp stains) and Xavi Franch Marro (3 Wg stains). For the dual stains, the level of each species was recorded separately in its own imaging channel. The Dpp stains suffered from significant saturation of pixels located at the Dpp source stripe. The experiment these stains were originally produced for was measuring low levels of expression far from the source stripe and so a high gain was used, resulting in saturation of most of the pixels in the source. Non-saturated Dpp data would obviously have been greatly preferred but none could be obtained within the time allocated for this case essay. Although care must be taken in the interpretation of the Dpp data, it can still be used to qualitatively visualise the profile of the Dpp distribution.

The raw 3D data from these scans was in the form of a "stack" of 2D images, each of which was a planar x-y slice at a different height (z) within the disc. Each set of raw data was flattened to a 2D maximum projection representation, where each point in the plane of the maximum projection was set to the maximum value at that point across all the z-slices.

Data visualisation

The disc image data was explored using a custom Matlab visualisation tool which permitted easy 2D and 3D visualisation of individual z-slices as well as various flattened projections of the stack. The visualisation tool also permitted various smoothing methods to be easily applied to the data.

All disc image data presented in this case essay is shown as a maximum projection representation. All projections have been normalised, as the fluorescence levels in the raw scan data reflect uncalibrated relative levels of expression. The normalised expression levels are represented by a "heat map" coding, where dark blue represents zero expression and dark red represents maximum expression. Pixels for which the original fluorescence data was saturated are marked in black to indicate that the true level of expression is uncertain at that point. Only the Dpp stains suffered from significant saturation.

In all 2D plots the projections are shown with no smoothing applied. In all 3D plots the projections have been smoothed with a normalised 2D Gaussian filter, with a standard deviation of 6px (Dpp data) or 3px (all other data). This filter size was chosen by eye for each data set in order to remove very short range variation and expose the longer range variation in the data more clearly. It is larger for the Dpp data as the spatial resolution of the images is greater.

Data smoothing

The raw disc image data contains lots of relatively high amplitude short range variation (see figure A1). Some considerable thought was given to how to smooth the raw data to reveal the underlying longer distance trend in the distribution of the target species. Four different smoothing methods were considered:

Averaging across multiple 1D cross-sections - This was rejected as it is essentially averaging 2D data along 1 dimension. It is clear from the 3D view of the raw image data in figure A1 that the high frequency variation is approximately uniform in all directions and therefore any smoothing technique should average over 2 dimensions.

Uniform averaging each pixel with its neighbours - This sort of "top hat" filter is formally equivalent to multiplying the image by a Sinc function in the frequency domain. This will periodically enhance and repress a range of frequencies across the spectrum and almost certainly introduce artefacts into the filtered image. While these artefacts may or may not affect the interpretation of the data, other methods will not introduce them at all and so this method was rejected.

Convolution with a Sinc filter - This would achieve the opposite of the uniform 2D average described above, multiplying the image by a "top hat" in the frequency domain. This is an ideal low pass filter, selectively removing all variation above a specified spatial frequency. However, due to the discrete nature of the image data (it is made of pixels) useful Sinc filters are very large. This makes them slow and, more importantly, vastly increases the area of the image subject to filtering edge effects (pixels near the image edge do not have a full neighbourhood).

Convolution with a Gaussian filter (Gaussian smoothing) - Convolution with a Gaussian filter replaces the value of each pixel with a 2D weighted average of its neighbourhood. This convolution is formally equivalent to multiplication by a (different) Gaussian in the frequency domain and acts as a "soft-edged" low-pass filter. This method was selected as it provides smooth filtering in the frequency domain with relatively small and fast filters. The effect of Gaussian smoothing is illustrated in figure A1.

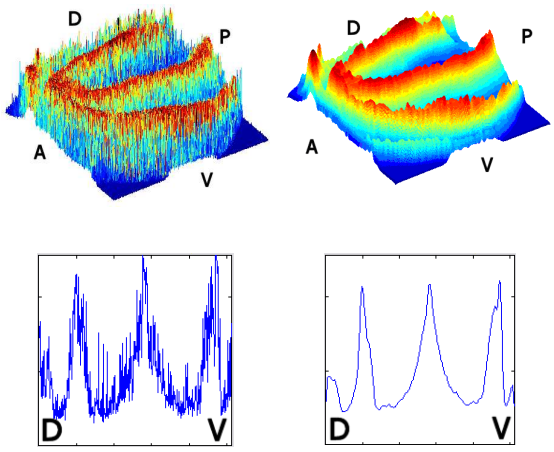

Figure A1: Comparison of raw and smoothed maximum projection representations of Wg expression. Top plots show 3D representation of Vg expression and bottom plots show a 1D cross-section across the A-P ridge, taken near the D-V compartment boundary which bisects the disc image. Smoothing with a Gaussian filter selectively damps the short range variation, exposing the long range variation more clearly.